Synthesis and Potential Applications of Graphene Nanoribbons

N. Kumara Swamy[1,2] and K. N Mohana[1]*
[1]Department of Studies in Chemistry, Manasagangotri,
University of Mysore, Mysuru-570006, Karnataka, India
[2]Department of Chemistry, JSS Science and Technology University,
Mysuru-570006, Karnataka, India
Phone: +91- 9449627573
* **Contact:** drknmohana@gmail.com

DOI: 10.3578/jecsi .68.1&2.2019.52

Abstract:

Graphene nanoribbons (GNRs) are the thin and elongated one-dimensional strips of graphene that possesses narrow widths and abundant edges. The edges are chemically more reactive and can be anchored with several chemical groups such as carboxyl, carbonyl and amines. Depending on the type of edge, width and chemical dopants involved, GNRs exhibit different chemical, optical, electrical and electronic properties**.** The presence of reactive edges in GNRs make them very potent materials for biosensing, corrosion prevention and water remediation applications while their tunable band gap structure make them ideal candidates for a variety of semiconductor based electronic, photonic and photovoltaic applications. In this article, the current state of research on the synthesis of GNRs, their properties and applications in the areas such as electrochemical biosensors, energy storage, opto-electric materials, water remediation, etc. has been reviewed. The review concludes that GNRs possess diverse tunable properties and most of their potentials are yet to be explored.

Key words: Graphene nanoribbon, Aspect ratio, Band gap, Energy storage, Biosensors

1. Introduction

Carbon-based materials have attracted the interest of research community owing to their extraordinary physical and chemical properties which make them suitable for many cutting-edge technological applications. Graphene nanoribbons (GNRs) exhibit exceptional electronic property, thermal stability and low percolation threshold (Han *et al.,* 2007; Li *et al.,* 2008; Son *et al.,* 2006). Recent theoretical and experimental works have demonstrated that GNR is a promising material for numerous applications such as energy generation and storage (Liu *et al.,* 2014a; Uthaisar and Barone, 2010; Wang 2015), chemical and biosensors (Hou *et al.,* 2014; Wang *et al.,* 2010), catalysis (Davis *et al.,* 2014; Holby and Taylor, 2012), and nanoelectronics (Fiori and Iannaccone, 2007; Wang *et al.,* 2008).

GNRs are the one-dimensional strips of sp^2 hybridized carbon crystal that possesses a large length to width ratio (aspect ratio) compared to graphene. In other words, GNRs are the thin, elongated strips of graphene that possess narrow widths and abundant edges. The width of GNRs ranges from sub-10 nm to several hundred nanometers while the thickness is about of several nanometers. (Cai *et al.,* 2010; Han et al., 2007; Kosynkin *et al.,* 2009; Ma *et al.,* 2013a; Shimizu *et al.,* 2011). Unlike graphene sheets that feature a zero bandgap, GNR possesses an open bandgap that can be controlled by tuning atomic-scale structures (Lin *et al* 2017). For example, GNR with designed edges can effectively modulate the electronic energy gap, thus enhancing the charge transfer and chemical reactivity when used for chemical and biological detection. The reduction

of graphene oxide nanoribbon (GONR) is a promising alternative for the bulk production of GNR-based materials because it can be synthesized in large quantities (Ma *et al.,* 2013b).

Classification

On the basis of the edge termination style, the GNRs are classified as armchair or 0æ% (A-GNRs) and zigzag or 30æ% nanoribbons (Z-GNRs), respectively. The schematic overview of GNRs is given in **Figure-1**.

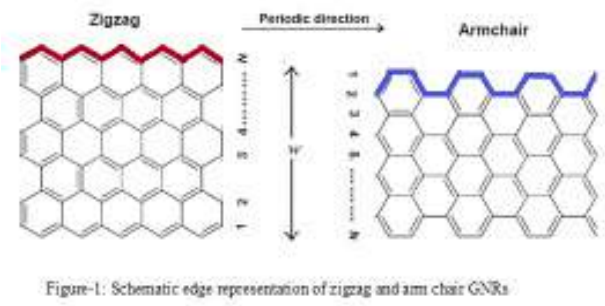


Figure-1: Schematic edge representation of zigzag and arm chair GNRs

Figure-1: Schematic edge representation of armchair and zigzag GNRs

The width of A-GNR is decided by the number of hexagonal carbon rings or generally referred as dimer lines (Na) across the ribbon where as the width of the Z-GNR is dependent on the number of zigzag chains (Nz) across the ribbon(Sharda and Agarwal, 2014). The termination styles are one of the factors which determine the electronic states of GNRs. According to tight binding model, Z-GNRs are metallic while armchair can be either metallic or semiconducting depending on width of GNRs (Rakheja et al. 2013).

2. Properties of GNRs

2.1. Edge and chemical characteristics

The non-functionalized GNRs show high solubility in chlorosulfonic acid but insoluble in most other solvents. GNRs are insoluble in water and they minimize their interaction with water molecules by forming a densely packed self-assembled film of stacked nanoribbons (Mehdi Pour et al. 2017).

GNRs surfaces appear to be chemically inert, and these surfaces usually interact with other molecules via physical adsorption (interactions) similar to graphenes. The properties of GNRs are dependent on edge type and the nature of edge substituent. Nanoribbons intrinsically have dangling bonds at the edges which provide active sites for chemical modification. Modifications can be done through several ways of functionalization such as functionalization by s-type, p-type, and d-type elements (Gorjizadeh et al., 2008; Wu et al 2010.; Lee 2010.; Kan et al. 2008), or by functional groups. Several chemical groups such as carboxyl (-COOH), carbonyl (-CO), hydrogenated (-CH) and amines (-NH_2) could be anchored at the edges of GNRs which are more chemically reactive (Terrones et al. 2010). In addition, the chemical reactivity could change drastically at these edges, depending on the nature of carbon termination, either armchair or zigzag (Terrones et al. 2010).

Substitution of one or more carbons of the nanoribbon by introducing impurities to the system is another effective way to control the electronic properties of the nanoribbons. Intrinsically boron (B) and nitrogen (N) impurities play the role of p-type and n-type doping in carbon-based materials. But, in nanoribbons the doping process is extremely sensitive to the dopant position and density, type and width of the ribbon (Yu et al., 2008; Biel et al., 2009). If B(N) substitution occurs in the center of the A-GNRs resulting in a semiconductor to metal transition (Cervantes-Sodi et al 2008) while the substitution at the edge position donot change the electronic properties of ribbon.

In case of Z-GNRs, the B and N substitution at the ribbon edges in Z-GNRs induce semiconductor to metal transition (Cervantes-Sodi et al 2008). Zheng et al. (2010) have shown that zigzag nanoribbons can be made semiconducting, half metallic or metallic by controlling the distance of the N or B impurity atoms to the edge. The substitution of one edge carbon with B atoms and the other edgecarbon with N atoms makes the ribbons half metallic. Half-metallicity can be also achieved either by replacing middle carbons of

zigzag nanoribbon by B-N chains ( ) (Dutta et al. 2009).

The installment of alkyl chains at the innermost positions of the cove-type edges can bend the peripheral rings of the GNR through steric repulsion between aromatic protons and the introduced alkyl chains. This structural distortion is theoretically predicted to reduce the bandgap by up to 0.27 eV, which is supported by experimental comparison of thus synthesized planar and non-planar GNRs through UV-Vis-near infrared absorption and photoluminescence excitation spectroscopy (Hu e et al., 2008). These results indicate that the electronic and optical properties of GNRs can also be modulated by introducing systematic and uniform deviations from planarity (Hu e et al., 2008).

2.2. Mechanical Properties

GNRs have shown to influence mechanical properties when used as fillers in polymer materials. The homogeneous dispersion of the GNR has shown to enhance the thermal stability and mechanical performance of the poly vinyl alcohol (PVA). A significant increase in the mechanical performance of the PVA/GNR nanocomposites is observed compared to pure PVA (Shang et al., 2015). The GNR and PVA matrix had shown very strong hydrogen bond interactions, the GNR shared some stress when the nanocomposite was stretched, resulting in a significant increase in the tensile strength of PVA/ GNR 1.0 wt % nanocomposite. Compared with the pure PVA, the tensile strength of the PVA/GNR 2.0 wt % nanocomposite increased by 85.7 % from 18.2 Mpa to 33.8 Mpa, and the Young's Modulus increased by 65.2 % from 705 Mpa to 1164 Mpa, although the tensile strain decreased to some extent. The typical strain–stress behavior of the PVA and the PVA/GNR nanocomposites is shown **Figure-2A.** The mechanical characteristics shown in **Table-1** indicate that the GNR was effective for various polymer nanocomposite applications. The mechanical studies on other polymeric and non-polymeric composites or hybrids are not available in literature.

Table-1: Tensile properties of the PVA and PVA/GNR nanocomposites (Shang *et al.,* 2015).

Samples	Tensile stress (MPa)	Tensile strain (%)	Modulus (MPa)
PVA	18.2	68.8	705
PVA/GNR 1.0 wt %	27.4	49.1	813
PVA/GNR 2.0 wt %	33.8	31.9	1164

2.3. Electronic properties

2.3.1. Band gap

The band gap is a key property of electronic materials and the size of the gap is decisive for the suitability of a material for electronic devices. The width of the gap depends on the ribbons edge configuration/chirality and width (number N of carbon atoms along the ribbon width). The results of theoretical calculations based on Green Wave function (GW) method showed that the band gap of both A-GNRs and Z-GNRs vary inversely with width of nanoribbons (Yang et al.2007). The experimental band gap values of armchair and zigzag GNRs obtained by scanning tunneling microscopy (STM) lithographic methods show a similar trends though there are certain derivations in the results which may be attributed to level of precision attainable over ribbon width and edge configuration in the synthesis process. This shows that the band gap is extremely sensitive to the ribbon width and edge configuration, both of which have to be controlled atomically precise if a certain band gap is needed (Yang et al.2007; Geng et al. 2017). The correlation between the band gap and width of GNRs is shown in **Figure-2B**.

2.3.1. Carrier mobility

The effective charge carrier mobility in electronic materials is vital for device development application. In conventional semiconductors, the tendency of decreasing mobility for increasing

band gap is observed. Unfortunately, the same trend is predicted by theory and observed experimentally for GNRs. The band gap opening in GNRs comes at the expense of a

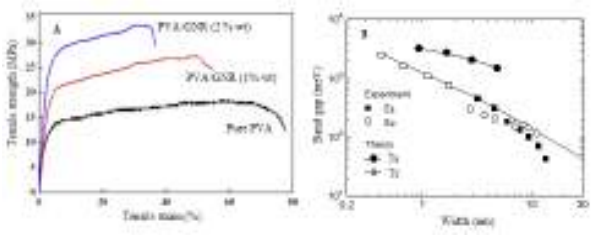


Figure-2: A) Typical stress-strain behavior of PVA and PVA/GNR nanocomposites (Shang et al., 2015). **B)** Variation of band gap of GNRs as a function of GNRs width. Experimental band gap of A-GNR (Ea) and Z-GNRs (Ez) fabricated by STM method. Theoretical band gap of A-GNRs (Ta) and Z-GNRs (Tz) (Yang et al.2017).

Table 2: Room temperature electron mobilities of graphene and GNRs (Geng *et al.* 2017).

Material	**Mobility (cm^2/Vs)**	**Remarks** (w is width)
LA graphene	200,000	Suspended graphene
	d" 40,000	Graphene on SiO_2
GNR	2500	w = 20 nm, suspended
	1500	w = 15 nm, on SIO_2
	64	w = 1.5 nm, on SIO_2
	100	w = 2 nm, on SIO_2
	190	w = 2.5 nm, on SIO_2
Si	1430	Bulk, undoped

degraded mobility (Schwierz., 2013; Schwierz, 2014). Carrier transport in GNRs not only depend on the properties of the ribbons themselves, but is affected to a large extent by the substrate as well. The data in **Table-2** reveal that the mobility in suspended large-area graphene is much larger than in graphene on SiO_2, and the same trend is observed for GNRs. Since suspended channels are difficult to implement into practical devices, a lot of work has been spent on realizing both large-area graphene and GNRs on substrates which minimize the degradation of carrier transport. The table also shows that the carrier mobility in GNRs vary directly with the width of GNRs and the GNRs wider than 15nm exhibit better carrier mobility vales compared to intrinsic silcon semiconductor.

2.4. Thermal properties

The thermal properties are important from the perspective of device performance of electronic industry. As the electronic industry moves toward nanometer designs, the thermal dissipation problem in electronic circuits has become one of the most important challenges (Vassighi *et al.,* 2006). A possible approach for solving the thermal problem is finding a material with high thermal conductivity, which can be integrated with Si complementary metal-oxide-semiconductor (CMOS) technology. Diamond and carbon nanotubes have been considered for such applications (Jin and Mavoori, 1998; Biercuk *et al.,* 2002). However, due to the large thermal contact resistance, they are not well suited for integration with CMOS. Different from the diamond and CNTs, GNRs can be naturally attached to heat sinks, and thus avoiding the problem of thermal contact resistance (Ghosh *et al.*2008). This suggests GNRs can be excellent material for thermal management in the CMOS devices and circuits. The investigations show that GNRs exhibit high thermal conductivities and long phonons mean free paths. The thermal conductivity is sensitive to the edge shapes, length, widths and strains of GNRs and it varies as a function of the length, width and strain (Guo *et al*. 2009). The thermal conductivity does not converge to a finite value with the increase of GNRs length up to 60 nm. The thermal conductivity is also very sensitive to the width of GNRs (i.e no. of atoms N). The thermal conductivity of Z-GNRs increases first and then decreases with the increasing in N, while, for A-GNR's thermal conductivity monotonously increases with N (Guo *et al.* 2009). The thermal conductivity as a function of GNR length and width is given in **Figure-3.** Combined with their

unique electronic properties, GNRs may be a suitable candidate in future CMOS nanodevices.

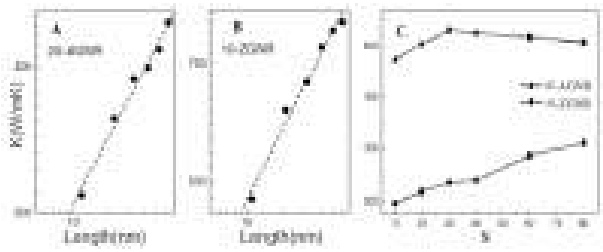


Figure-3. A) and **B**) Thermal conductivity, K (W/mk) vs length (nm) in log-log scale for 20-AGNR and 10-ZGNR. **C)** Variation of thermal conductivity, K vs length of GNR (N atoms) (Guo *et al.* 2009).

2.5. Optical properties

The optical behavior of GNRs depends on their structural purity (Senkovskiy *et al*. (2017) investigated the optical properties of GNRs. When GNRs are illuminated with 440 nm wavelength light in a laser scanning confocal microscope under ambient conditions, weak emission without distinct spectral features is observed. For defect-free sample of GNRs, the photoluminescence (PL) is expected to be dark. But, on continuous exposure of sample to 440 nm radiation, the emission brightens after 1 min, and a peak emerges at about 1.8 eV in the spectrum. This change in photo luminescent behavior is attributed to the increased emission due to the generation of defects in GNRs via a photochemical reaction. It is observed that the sample must be exposed to light with wavelengths shorter than approximately 510 nm for defect generation. For longer wavelengths, the PL remains dim independent of the photon energy used to excite PL. However, once the defects are generated, the emission spectrum remained same for all excitation wavelengths in the range of 420 to 590 nm indicating that the observed emission originates from an energetically well defined optical transition (Senkovskiy *et al*. 2017) These observations open interesting perspectives for the use of GNRs as near-infrared emitters. Nevertheless, the photoluminescence properties of GNRs have largely remained unexplored and still there is lot of scope for investigation as optical properties depends on many features such as edge configuration, doping type, dopant concentration and width of GNRs (Zhao et al. 2017).

3. Synthesis of GNRs

The synthetic methods employed in synthesis of GNRs are based on two approaches: a) Top-down and b) Bottom-up approach (Lukas *et al.* 2011). The schematic overview of top down and bottom up approaches is given in **Figure-4.**

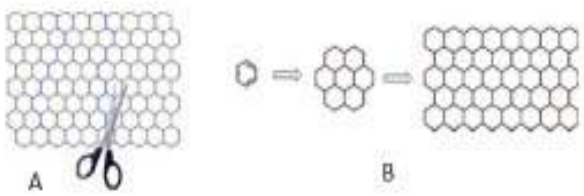


Figure-4: Schematic overview of **A**) Top down and **B**) Bottom-up fabrication of GNRs

In top-down approach the higher carbon based materials are cut or broken down into nanoribbons. The methods such as sonication, chemical cutting, chemical etching, scanning tunneling microscopy (STM), lithographic methods, etc., are employed in this approach. However, it is highly challenging to produce high-quality, narrow GNRs by these methods as the smooth edges produced by these methods are not precise at the atomic level and can entail undefined structural disorders, defects and errors of 1 nm or larger (Lukas *et al.* 2011). In bottom-up approach, the GNRs are produced by building or assembling or aggregating smaller chemical units into GNRs (Lukas *et al.* 2011). The bottom-up methods mainly include chemical vapor deposition and several chemical synthetic methods.

Some of the efficient synthetic methods are discussed below.

3.1. Growth using catalyst

This is one of the earliest methods demonstrated as early as 1990 (Lherbier et al. 2008). In this method, the multilayer GNRs with limited widths are grown on metal or carbide nanoclusters using iron carbide catalyst in chemical vapour deposition process. This process yields

nanoribbons with dimensions of 10 ì m long, 100–700 nm wide and 10–200 nm thick with an iron carbide particle at the end.

3.2. Growth on gold or silver surfaces

In this approach, the GNRs are grown by coupling of precursor hydrocarbon molecules into chains at silver or gold surfaces (Cai et al.2010). In these experiments, the precursor hydrocarbon molecules with two halogen end groups are deposited from a Knudsen cell on a gold or silver surface at about 200 °C. At this deposition temperature, the halogen atoms are removed from the precursor molecules, yielding bi-radical species which form the building blocks for chain molecules. As the radicals diffuse across the surface, they undergo radical addition reaction. Subsequent annealing at higher temperatures around 450 °C result in surface assisted cyclodehydrogenation reaction which yield an extended fully aromatic system. This process produced GNRs of uniform width with armchair edges. This is a promising method for synthesizing GNRs with well controlled and predefined properties (Batzil, 2012). However, the major challenge for practical application may be the scalability of the process and the controlled transfer of the ribbons into devices.

3.3. Cutting graphene with catalysts

In this method, the graphene sheets are cut into narrow GNRs using catalysts. The metals clusters of Ni (Miyamoto *et al.*1994; Hernandez *et al.* 1998) or Fe (Weng Sieh *et al.*1995) are first deposited onto graphene and heated in a hydrogen atmosphere. The metal acts as a catalyst to promote hydrogenation reactions as follows:

$$C(s) + 2H_2 \xrightarrow{Ni/Fe} CH_4(g)$$

This cutting process yields straight edged GNRs determined by the crystallographic orientation of graphene. It observed that preferential zigzag or armchair edges can be obtained depending on the metal cluster size (Hernandez *et al.* 1998).

3.4. GNR Synthesis by unzipping of carbon nanotubes

Jiao et al. (2009) and Kosynkin et al. (2009) have successfully synthesized graphene nanoribbons by unzipping multiwalled carbon nanotubes (MWCNTs). The width of the nanoribbons thus produced depends on the diameter of the precursor nanotubes. Dai et al. first embedded multiwalled CNTs in a PMMA film and then exposed this film to Ar plasma for various times so as to etch out top exposed portions of tube walls thereby opening up the tubes. They produced GNRs with reduced thickness i.e, reduced number of layers by varying exposure time.

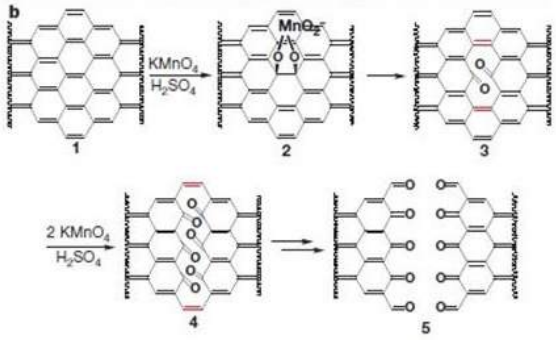


Figure-5: Mechanism involved in synthesis of GNRs by unzipping of carbon nanotubes.

The group of Kosynkin et al. (2009) opened up the MWCNTs by oxidizing them in presence of sulphuric acid and potassium permanganate. It was observed that the severity of oxidation increased with the concentration of $KMnO_4$ and this led to oxidation of more layers of MWCNTs. The nanoribbons produced were of graphene oxide and contained a lot of hydroxyl and epoxy groups. However, they could be reduced back to graphene using hydrazine and high temperature hydrogen annealing. The mechanism involved in longitudinal unzipping of MWCNTs is shown **Figure-5**.

3.5. Unzipping of MWCNT by mechanical sonication

The unzipping of multiwalled carbon nanotubes to GNRs can be achieved by mechanical sonication process. In this process, MWNTs are first calcinated at 500 °C in 1 inch tube furnace for 2 h and mixed with a polymer PmPV i.e, poly(m-phenylenevinylene-co-2,5-

dioctoxy-p-phenylenevinylene), which is finally dissolved in dichloroethane and sonicated for about an hour. The solution is later ultra-centrifuged at 40,000 rpm for 2 h and the supernatant which contain 60% nanoribbons is collected and dried (Jiao et al. 2010).

3.6. GNRs from graphene sheets by sonochemical method

In this technique, the graphene sheets are first dispersed in a mixture of polyvinylpyrrolidone and sodium dodecyl sulphate to form a stable homogenous suspension by sonication for 1 hour. The mixture is further treated with hydrazine hydrate and refluxed at 100 ^{o}C for 2 days. Later, the mixture is subjected to centrifugation to separate the GNRs (Wu et al. 2010).

3.6. Chemical exfoliation

In chemical exfoliation, GNRs are produced from 3D graphite by subjecting it to annealing at 1000 ^{o}C followed by sonication for 30 mins in a solution of dichloroethane and a polymer. GNRs obtained are separated from the reaction mixture by centrifugation (Li et al. 2008).

3.7. Chemical vapour deposition (CVD) method

In CVD method, a spray (atomized droplets) of ferrocene in ethanol, with thiophene, is carried by Ar gas to a hot furnace at 950 æ%C. The reaction under hot conditions produced nanoribbons of several micrometers long, 20-300 nm wide and less than 15 nm thick (Terrones et al. 2010).

3.8. Suzuki-Miyaura coupling reactions

Small GNRs can be synthesized by organic chemistry approaches linking tetra- and hexa-phenyl benzenes through the Suzuki-Miyaura reaction (Yang et al. 2008). The poly phenylene formed is then subjected to a cyclodehydrogenation reaction with $FeCl_3$ as the oxidant, which result in formation of ribbons with 6-12 polycyclic aromatic repeating units. This is a true bottom-up approach to thin and short GNRs with armchair edges.

3.9. Diel's Alder polymerization

Diels–Alder (D-A) polymerization route can be used for preparing tailor made polyphenylenes which can serve as precursors for the preparation of structurally well-defined GNRs with different widths, long lengths (up to 4600 nm) and tunable electronic bandgaps. The solution protocols for GNRs synthesis typically begin with the D–A polymerization of tailor made monomers which give rise to structurally well-defined polyphenylenes. These polyphenylenes are straight forwardly converted to GNRs by intramolecular oxidative cyclodehydrogenation (Hou et al. 2018).

3.9.1. A_2B_2-type D–A polymerization

Hou et al. (2018) developed a reaction scheme to synthesize GNRs using A_2B_2 type D-A polymerization (Scheme in **Figure-6**). They reacted 1,4-diethynyl-2,5-di(4'-tert-butylphenyl) benzene (**1**) with 4,4'-(1,4-phenylene)bis(2,3,5-triphenylcyclopenta-2,4-dien-1-one) (**2**) to achieve A_2B_2-type D–A polymerization, producing the tert-butyl-substituted polyphenylene (**3**). On planarization of this polymer through oxidative treatment with $FeCl_3$ in nitromethane, armchair GNR (**4**) is formed. However, the lengths of these GNRs are limited because of the difficulty in perfectly controlling the stoichiometry of the two different monomers used for polymerization. This limitation is detrimental for the fabrication of single-GNR-based devices.

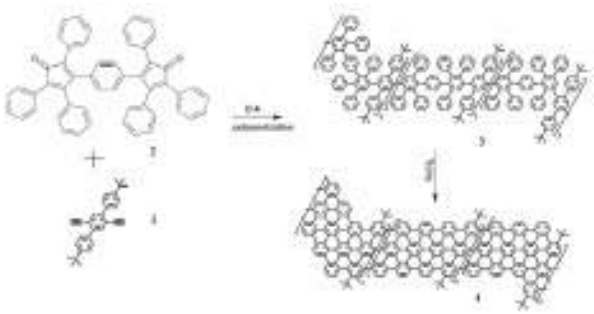


Figure-6: Synthesis of GNRs through A_2B_2-type Diel's Alder polymerization (Hou et al. 2018).

3.9.2. AB-type D–A polymerization

The difficulty in controlling the stochiometry can be reduced to get longer GNRs by adopting AB-

type D–A polymerization approach rather following A_2B_2-type approach (Hou et al. 2018). This approach was reported by the above group to produce 'cove'-type GNRs. The monomers having a cyclopentadienones (**5**) as the conjugated diene and an ethynyl group as the dienophile, are subjected to D–A polymerization to produce the alkylated polyphenylene precursor (**6**) which on intramolecular oxidative cyclodehydrogenation with $FeCl_3$ as the oxidant produce GNRs (**7**). The reaction scheme is shown in **Figure-7**. The alkylated polyphenylenes fabricated by the AB-type D–A polymerization protocol, giving unprecedented lengths of up to 600 nm (Hou et al. 2018) as determined from the molecular weight of their alkylated polyphenylene precursors. The degree of polymerization (GNR length) was significantly larger than those of polyphenylene precursors produced by A_2B_2-type D–A polymerization and other metal-catalyzed coupling reactions such as the Suzuki and Yamamoto polymerizations.

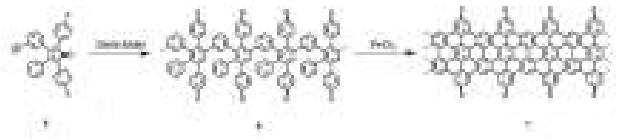


Figure-7: Synthesis of GNRs through AB-type Diel's Alder polymerization (Hou et al. 2018).

Finally, D–A polymerization offers a promising approach toward high-degree polymerized polyphenylenes precursors for bottom-up GNR synthesis. In particular, AB-type D–A polymerization furnished GNRs with an unprecedented length of over 600 nm, which surpassed GNRs constructed by other reactions, including metal-catalyzed aryl–aryl coupling, which typically possess lengths up to 100 nm. Furthermore, the width of the GNRs can be modulated by expanding the monomer structure, allowing tuning of their optoelectronic properties. Nevertheless, successful GNR synthesis through the AB-type D–A reaction is thus far limited to monomers based on ethynyl-substituted cyclopentadienones. Therefore, the next challenge should be the design of new AB-type monomers equipped with different dienes and dienophiles for synthesizing a greater variety of GNRs with unique structures, heteroatom doping and/or added functional groups, while preserving the length exceeding 100 nm. It is especially desirable to synthesize low-band gap GNRs with infrared absorption without broadening the ribbons.

4. Applications of GNRs

The survey of literature shows that the exciting edge chemistry and physics of the carbon based nanoribbons is expected to lead to many potential applications in the areas of novel catalytic reactions, sensor fabrication, the production of field effect transistors, the generation of electrodes for batteries, the assembly of heavy metal filters, the fabrication of highly conducting, transparent polymer composites and other composites with metals and ceramics, drug deliverers, etc (Terrones et al. 2010. Tiwari et al. 2016). However, controlled defect and edge engineering is needed in order to fine tune the chemical, electronic, mechanical, magnetic and thermal properties of nanoribbons (Terrones et al. 2010).

4.1. Biosensing

GNRs serve as excellent materials for electrochemistry and these materials show a large electrochemical potential window (approximately 2.5 V in 0.1mM phosphate buffer saline solution), the detection of molecules with either high oxidation or reduction potentials becomes feasible (Lin et al.2015). Further, the extremely high surface area provides an effective reaction area and a high capacity for enzyme loading. The presence of abundant edges and defects on these materials provide a high electron transfer rate suggesting that these materials are very suitable for electrochemical detection. The presence of numerous chemical moieties (hydroxy and carboxyl groups) on the surface afford flexibility and convenience for functionalization to enhance sensor performance (Liu et al. 2009). GNRs/GONRs based nanomaterials are ideal immobilization matrix owing to their large surface area, high conductivity, biocompatibility, high stability, good adhesion, inertness, affordability, physical strength, regenerability, ability to increase enzyme specificity/activity and hindrance to product inhibition and nonspecific adsorption.

Additional electrocatalyst such as, metal nanoparticles, metal oxides, polymers and other nanomaterials are attached on GONRs/GNRs surfaces to enable additional sensitivity and selectivity (Umamaheshwari et al. 2018).

The oxidized and reduced GNRs have been explored as sensor electrode materials for the detection of ascorbic acid, L-DOPA and uric acid in standard samples (Martin et al. 2015; Akbari and Buntat, 2015; Ismail et al. 2014; Jaiswal et al. 2015). The sensor developed using reduced GNRs on screen printed platforms showed improved performance than those developed using carbon paste electrode, MWCNTs and oxidized GNRs (Martin et al. 2015). Akbari and Buntat (2015) modeled and investigated CO_2 adsorption effects on GNR conductance and concluded that the GNRs can be used for the development of CO_2 gas sensor. The graphene based nanoribbons have also been used in the development of non-enzymatic electrochemical glucose sensor (Ismail et al. 2014). Another study showed that the edges of zigzag GNR can be reconstructed to effectively sense nitrogen based molecules such as ammonia (Jaiswal et al. 2015). However, the biosensing applications of carbon based nanoribbons have not been explored much to their full potential as these materials are relatively new.

A highly sensitive (sub-nanomolar level) methyl parathion sensor is fabricated using Ag@GNRs/SPCE and its practical applicability is successfully demonstrated in food samples such as cabbage, green beans, strawberry and nectarine samples (Umamaheshwari et al. 2018). An ultra-sensitive, reproducible, stable and practically applicable modified electrode based on electrochemically reduced (ER)-GONRs is fabricated for the determination of nimesulide, a non-steroidal anti-inflammatory drug. The sensor exhibited wide linear range (1.0×10^{-8}– 1.50×10^{-3} nM), low detection limit (3.50 nM), high sensitivity (1.20 ìA. ìM^{-1}.cm^{-2}) and fast response (< 5 s) towards nimesulide detection (Govindasamy et al. 2017).

Guanine is electrochemically immobilized on GNR modified electrode, which is used as a DNA biosensor for the evaluation of total antioxidant capacities (TAC) in fruit juices (Yang et al. 2013). A label-free impedimetric aptasensor that detects femto molar level of acetamiprid is developed using Au decorated MWNTs/reduced GONR composite (Fei et al.2015). A third generation glucose biosensor was developed based on wiring of apo-enzyme of glucose oxidase with GNR bound to FAD at a screen-printed carbon electrode (Mehmeti et al.2017).

4.2. Electronics devices

The electronic properties GNRs differ from graphene because as the number of carbons decreases there is splitting of the HOMO and LUMO resulting in larger band gaps as GNRs become thinner. Density functional theory has predicted that the electronic properties of GNRs differ with changes in length, width and differences in edge structure (Johnson, 2013). GNRs exhibit tunable band gap structure which makes them ideal candidate for a variety of semiconductor based electronic, photonic and photovoltaic applications (Timothy et al. 2014).

The non-zero band gap of GNRs makes them very potential material for electronic applications. Field emission transistor (FET) is a semiconductor based electronic device. A typical FET device consists of a semiconductor layer, a dielectric layer, a gate electrode and source–drain (S–D) electrodes. The current flow between the S–D electrodes (drain current) can be controlled by a voltage applied to the gate electrode (gate voltage) (Ma et al. 2013b). Inorganic materials, especially silicon, have been predominantly employed for the semiconductor layer, but alternative materials such as organic semiconductors (Horowitz, 1998; Muccini, 2006; Di et al. 2007) as well as graphene and related materials (Avouris and Chen, 2006) are recently attracting more and more attention.

A field effect transistor (FET) biosensor is developed using solution-processed GONRs and the sensor is applied in sensing methylene blue (Lin et al. 2017) and adenosine triphosphate (Dong et al. 2011). Studies revealed that GNRs possess intrinsic peroxidase-like catalytic activity and hence it is a desired material for biosensing

applications (Qian et al. 2015). GNRs based nanocomposites are reported to be biocompatible and suitable for immobilizing bio-receptors such as, biomolecules, antibodies, aptamers etc. (Liang et al. 2017).

4.3. Energy storage devices

The presence of structural defects and some oxgen containing functional groups in GNRs can generate pseudo-capacitance and also improve electrolyte ionic accessibility. The longitudinal unzipping increases effective surface area, thus releases more electroactive sites of GNRs for fast electrochemical reactions. These characteristics are highly desired in energy storage devices like batteries and super-capacitors. Li et al. (2016) prepared a SnO_2@TiO_2/GNRs nanocomposite and used it as electrode material in lithium ion battery. This composite exhibited high discharge capacity, high reversible capacity and excellent cyclability and rate capability. They concluded that GNRs obtained from unzipping CNTs is a promising anode material for lithium ion batteries. Xiao et al. (2014) have used GNRs obtained at different stages of unzipping CNTs and tested their performance as electrode material in lithium storage battery. The galvanostatic charge-discharge studies revealed that increase of defect enhances the capacity in early stages of unzipping process while it fades in final stages of completion of unzipping process. They found that the performance can be optimized by having control in the defect structures in GNRs at the time of preparation. Li et al. (2015) used GNRs unzipped from MWCNTs as super-capacitor electrode material and found that GNRs exhibit much higher super-capacitor performance than the pristine MWCNTs.

4.3. Photovoltaics

There are also some reports available on the use of GNRs for the development of counter electrode in dye sensitized solar cell (DSSC) applications (Min-Hsin et al. 2014, Yang et al. 2013, Xue et al. 2015). Xue et al (2015) prepared N-doped GNRs by thermal method and used them as efficient metal free counter electrodes for disulfide/thiolate redox mediated DSSCs. The developed solar cell showed better performance compared to conventional platinum counter electrode. Min-Hsin et al. (2013) prepared a catalytic film of MWCNTs with reduced GONR and used it as a counter electrode in DSSC. The developed DSSC achieved about 7.2 % photo conversion efficiency which is better than the efficiency of pristine MWCNT. Yang et al. (2013) bridged CNT with GNRs and employed them in fabrication of counter electrode in DSSC which resulted in an efficiency of 8.23 % as against 7.6 % of conventional platinum counter electrodes. The results of these studies indicate that the GNR based counter electrodes fare better than conventional platinum electrode and therefore act as efficient electrode materials for DSSCs. However, many more studies involving GNRs and or their different functional forms are essential to exploit the full potentials of GNRs as solar cell electrode materials.

4.4. Corrosion and water remediation

The presence of chemically modifiable edge groups in GNRs provide ample of opportunities for the manipulation of its surface leading to altered surface characteristics. The surfaces suitable for many anticorrosive and water treatment applications can be readily engineered through modification of edge groups. This provides an opportunity to use GNRs as efficient anticorrosive and water remediation material. However, there is dearth of literature related to examination of water treatment and corrosion inhibition potentials of GNRs.

5. Conclusions and future directions

The fact that GNRs exhibit diverse properties which suit various applications makes them attractive materials for research. An impediment for realizing GNR based electronics is opening up of band gap without affecting other electronic properties. The persisting issues of polydispersity and dimension control come into picture with nanoribbon formation. Thus, a major breakthrough is desired in the synthesis of GNRs with controlled edge structures, width and chirality. Once these problems are addressed, GNR based electronics should become a reality in the future. The literature

also show that there is lot of scope for future work to explore the application potentials of GNRs in areas such as biosensing, corrosion prevention, water remediation, catalytic or photovoltaic applications.

References:

Akbari E and Buntat Z, Electronic Letters, 51(14), 1092-1094, (2015).

Batzill, M., Surface Science Reports, 67, 83–115 (2012).

Biel, B., X. Blase, F. Triozon, and S. Roche, Physical Review Letters, 102(9), 096803-096803, (2009).

Biercuk, M. J., M. C. Llaguno, M. Radosavljevic, J. K. Hyun, and A. T. Johnson, Applied Physics Letters, 80, 2767-2769, (2002).

Cai, J.M., Ruffieux, P.,Jaafar,R.,Bieri,M.,Braun,T.,Blankenburg,S.,Muoth,M., Seitsonen, A.P.,Saleh,M.,Feng,X.L.,Mullen,K.,Fasel,R., Nature, 466 (7305), 470–473, (2010).

Cervantes-Sodi, F., G. Cs´anyi, S. Piscanec, and A. C. Ferrari, Physical Review B, 77(16), 165427-165440, (2008).

Davis, D.J., Raji, A.R.O., Lambert, T.N., Vigil, J.A., Li, L., Nan, K., Tour, J.M., Electroanalysis 26(1), 164–170, (2014).

Dong, X., Q. Long, J. Wang, M.B. Chan-Park, Y. Huang, W. Huang, P. Chen, Nanoscale, 3 5156-5160, (2011).

Dutta, S., A. K. Manna, and S. K. Pati, Physical Review Letters, 102(9), 096601-096605, (2009).

Fei, A., Q. Liu, J. Huan, J. Qian, X. Dong, B. Qiu, H. Mao, K. Wang, Biosensors. Bioelectronics, 70, 122-129, (2015).

Fiori, G., Iannaccone, G., IEEE Electron Device Letters, 28(8), 760–762. (2007).

Geng,Z., Bernd H¨ahnlein, Ralf Granzner, Manuel Auge, Alexander A. Lebedev, Valery Y. Davydov, Mario Kittler, J¨org Pezoldt, and Frank Schwierz, Annlender. Physics, 529, 1700033-1700048, (2017).

Ghosh, IS., Calizo, D. Teweldebrhan, E. P. Pokatilov, D. L. Nika, A. A. Balandin, W. Bao, F. Miao, and C. N. Lau, Applied Physics Letters, 92, 151911, (2008).

Govindasamy, M., V. Mani, S.-M. Chen, T. Maiyalagan, S. Selvaraj, T.-W. Chen, S.-Y. Lee, W.-H. Chang, RSC Advances, 7, 33043 (2017).

Gorjizadeh, N., A. A. Farajian, K. Esfarjani, and Y. Kawazoe, Physical Review B, 78(15), 155427-155413, (2008).

Guo, Z., Dier Zhang, and Xin-Gao Gong, Applied Physics Letters, 95, 163103, (2009).

Han, M.Y., Özyilmaz, B., Zhang, Y., Kim, P., Physical Review Letters. 98(20), 206805 (2007).

Hernandez, E., C. Goze, P. Bernier and A. Rubio, Physical Review Letters, 80, 4502 (1998)

Holby, E.F., Taylor, C.D., Physical Review Letters, 101 (6), 064102 (2012).

Hou, Y., Li, J., Wen, Z., Cui, S., Yuan, C., Chen, J., Nano Energy, 8, 157–164 (2014).

Hou. Y., Yunbin Hu, Akimitsu Narita and Klaus Müllen, Polymer Journal, 50, 3–20 (2018).

Hu, Y., et al., Journal of American Chemical Society, Just Accepted Manuscript • DOI: 10.1021/jacs.8b02209, (2018)

Ismail, N., Quynh Hoa Le et al, Electro Chimica Acta, 146, 98-105 (2014).

Jaiswal, N. K., Goran Kovacevic, Branko Pivac, Applied Surface Science, 357, 55-59 (2015).

Jin, S., and H. Mavoori, Journal of Electronic Materials. 27, 1148, 1998.

Jiao, L. Y., L. Zhang, X. R. Wang, G. Diankov and H. J. Dai, Nature 458, 877 (2009)

Jiao, L., Xinran Wang, Georgi Diankov, Hailiang Wang and Hongjie Dai, Nature. Nanotechnology, 5, 321-326 (2010).

Johnson C.R., MA Thesis, The University of Texas at Austin, (2013).

Kan, E.-J., Z. Li, J. Yang, and J. G. Hou, Journal of the American Chemical Society, 130 (13), 4224–4225, (2008).

Kosynkin, D.V..Higginbotham, A.L.Sinitskii, A.Lomeda, J.R.Dimiev, A.Price, B.K. Tour, J.M.Nature, 458 (7240), 872–876 (2009).

Lee, Y.L., S. Kim, C. Park, J. Ihm, and Y.-W. Son, ACS Nano, 4(3),1345–1350, (2010).

Li, X.,Wang,X.,Zhang,L.,Lee,S.,Dai,H., Science, 319 (5867), 1229–1232 (2008).

Li, J., Senbin Ye, Tongtao Li , Xinlu Li, Xiaohan Yang, S. Ding, Procedia Engineering, 102, 492-498 (2015).

Li, X., Xinlin Zhang, Ronghua Wang, Zelong Su, Junwei Sha, Pengfu Liu, Journal of Power Sources 336, 298-306 (2016).

Liang, Y. R., Z.-M. Zhang, Z.-J. Liu, K. Wang, X.Y. Wu, K. Zeng, H. Meng, Z. Zhang, Biosensors and Bioelectronics, 91, 199 (2017).

Lin, J., Zhen Liu, Colin J. Barrow, Wenrong Yang, Analytica Chemica Acta, 859, 1–19 (2015).

Lin, T., Yan-Sheng Li, Wei-Hung Chiang, Zingway Pei, Biosensors and Bioelectronics, 89, 511–517, (2017).

Liu, J., Durstock, M., Dai, L., Energy Environmental Science, 7(4), 1297–1306. (2014),

Liu, Z.-B. Xu, Y.-F. Zhang, X.-Y. et al, Journal of Physical Chemistry B, 113, 9681–9686 (2009).

Lherbier, A., X. Blase, Y. M. Niquet, F. Triozon and S. Roche, Physical Review Letters, 101, 036808, (2008).

Lukas D, Lileta Gherghel, Xinliang Feng, and Klaus M_llen, Angew Chemistry. 50, 2540–2543. (2011).

Ma, L.,Wang, J., and Ding, F.,. Chem Phys Chem, 14(1),47–54, (2013a)

Ma, L.,Wang, J. L., Ding, F., Chem Phys Chem, 14(1), 47–54, (2013b).

Martín, A., Hernández-Ferrer, J., Martínez, M. T., and Escarpa, A. Electrochimica Acta, 172, 2-6, (2015).

Pour, M. M., Lashkov, A., Radocea, A., Liu, X., Sun, T., Lipatov, A., and Sysoev, V. Nature Communications, 8(1), 820, (2017).

Mehmeti, E., Stankoviæ, D. M., Chaiyo, S., Zavasnik, J., •agar, K., and Kalcher, K. Microchimica Acta, 184(4), 1127-1134, (2017).

Yeh, M. H., Lin, L. Y., Sun, C. L., Leu, Y. A., Tsai, J. T., Yeh, C. Y., and Ho, K. C. The Journal of Physical Chemistry C, 118(30), 16626-16634. (2014).

Miyamoto,Y., Rubio, A., Cohen, M. L., and Louie, S. G., Physical Review B, 50(7), 4976, (1994).

Qian, J., Yang, X., Yang, Z., Zhu, G., Mao, H., and Wang, K. Journal of Materials Chemistry B, 3(8), 1624-1632, (2015).

Schwierz, F. Graphene transistors. Nature nanotechnology, 5(7), 487, (2010).

Schwierz, F. Graphene transistors: status, prospects, and problems. Proceedings of the IEEE, 101(7), 1567-1584, (2013).

Senkovskiy, B. V., Pfeiffer, M., Alavi, S. K., Bliesener, A., Zhu, J., Michel, S., and Petaccia, L. Nano letters, 17(7), 4029-4037, (2017).

Shang, S., Gan, L., Yuen, C. W. M., Jiang, S. X., and Luo, N. M. Composites Part A: Applied Science and Manufacturing, 68, 149-154, (2015).

Sharda, V., and Agarwal, R. P. IEEE Recent Advances in Engineering and Computational Sciences (RAECS), 1-6, (2014).

Son, Y. W., Cohen, M. L., & Louie, S. G. Nature, 444, 347–349, (2006).

Shimizu, T., Haruyama, J., Marcano, D. C., Kosinkin, D. V., Tour, J. M., Hirose, K., and Suenaga, K. Nature nanotechnology, 6(1), 45, (2011).

Terrones, M., Botello-Méndez, A. R., Campos-Delgado, J., López-Urías, F., Vega-Cantú, Y. I., Rodríguez-Macías, F. J., and Terrones, H. Nano Today, 5(4), 351-372, (2010).

Vo, T. H., Shekhirev, M., Kunkel, D. A., Morton, M. D., Berglund, E., Kong, L., and Sinitskii, A. Nature Communications, 5, 3189, (2014).

Tiwari, J. N., Vij, V., Kemp, K. C., and Kim, K. S, ACS Nano, 10(1), 46-80, (2015).

Rajaji, U., Arumugam, R., Chen, S. M., Chen, T. W., Tseng, T. W., Chinnapaiyan, S., and Chang, W. H., International Journal of Electrochemical Science, 13, 6643-6654, (2018).

Uthaisar, C., & Barone, V. Nano Letters, 10(8), 2838-2842, (2010).

Vassighi, A., & Sachdev, M. Springer Science & Business Media, (2006).

Wang, X., Ouyang, Y., Li, X., Wang, H., Guo, J., and Dai, H., Physical Review Letters, 100(20), 206803,(2008).

Wang, Y., Shao, Y., Matson, D. W., Li, J., and Lin, Y. ACS Nano 4, 1790–1798, (2010).

Wang, C., Li, Y. S., Jiang, J., and Chiang, W. H. ACS applied materials & interfaces, 7(31), 17441-17449, (2015).

Weng Sieh, Z., K. Cherrey, N. G. Chopra, X. Blase, Y. Miyamoto, A. Rubio, M. L. Cohen, S. G. Louie, A. Zettl and R. Gronsky, Physical Review B 51, 11229 (1995).

Wu, M., Wu, X., & Zeng, X. C. The Journal of Physical Chemistry C, 114(9), 3937-3944, (2010).

Wu, Z. S., Ren, W., Gao, L., Liu, B., Zhao, J., & Cheng, H. M. Nano Research, 3(1), 16-22, (2010).

Xue, Y., Chen, H., Qu, J., and Dai, L. 2D Materials, 2(4), 044001, (2015).

Yang, L. L. Yang, C.-H. Park, Y.-W. Son, ML Cohen, and SG Louie, Physical Review Letters, 99, 186801, (2007).

Yang, Z., Liu, M., Zhang, C., Tjiu, W. W., Liu, T., and Peng, H. Angewandte Chemie International Edition, 52(14), 3996-3999, (2013).

Yu, S. S., Zheng, W. T., Wen, Q. B., and Jiang, Q. Carbon, 46(3), 537-543, (2008).

Yang, X., Dou, X., Rouhanipour, A., Zhi, L., Räder, H. J., and Müllen, K. Journal of the American Chemical Society, 130(13), 4216-4217, (2008).

Zhao, S., Rondin, L., Delport, G., Voisin, C., Beser, U., Hu, Y., and Lauret, J. S., Carbon, 119, 235-240, (2017).

Zheng, X. H., Wang, X. L., Abtew, T. A., & Zeng, Z. The Journal of Physical Chemistry C, 114(9), 4190-4193, (2010).